Missing one-loop contributions in secondary gravitational waves

Chao Chen,[1,*] Atsuhisa Ota,[1,†] Hui-Yu Zhu,[1,2,‡] and Yuhang Zhu[1,2,§]

[1]*Jockey Club Institute for Advanced Study, The Hong Kong University of Science and Technology, Clear Water Bay, Kowloon, Hong Kong, People's Republic of China*

[2]*Department of Physics, The Hong Kong University of Science and Technology, Clear Water Bay, Kowloon, Hong Kong, People's Republic of China*

(Received 13 November 2022; accepted 20 March 2023; published 19 April 2023)

We find several missing one-loop-order contributions in previous considerations about secondary gravitational waves induced at nonlinear order in cosmological perturbations. We consider a consistent perturbative expansion to third order in cosmological perturbations, including higher-order interactions and iterative solutions ignored in the previous literature. Tensor fluctuations induced by the source with two scalar and one tensor perturbations are correlated with the first-order tensor fluctuation and thus give a one-loop order correction to the tensor-power spectrum. The missing loop correction is *scale invariant* and *negative* in the superhorizon region, which secondarily reduces the initial primordial tensor-power spectrum prior to the horizon reentry. Such an IR behavior is very different from the autospectrum of second-order induced tensor modes discussed in the previous literature and can be important for the actual gravitational wave measurements. For a sharp peak of scalar fluctuations with $A_\zeta = 10^{-2}$ at $k_* = 10^5\, h/\mathrm{Mpc}$ motivated by the LIGO/Virgo events, we show that the tensor-power spectrum at the cosmic microwave background scale reduces by at most 35%. Hence, the polarization B mode might not be seen because of the reduction of the original tensor spectrum due to the secondary effect of primordial black hole formation.

DOI: 10.1103/PhysRevD.107.083518

I. INTRODUCTION

The direct detections of gravitational waves (GWs) from the binary black hole/neutron star mergers break new ground in physical cosmology [1,2], marking a new era of the multimessenger astronomy by combining GWs, electromagnetic and neutrino observations [3]. The interaction between GWs and matter is weak. Hence, GWs propagate almost freely through the Universe and carry unique astrophysical and cosmological information. The primordial gravitational waves (PGWs) produced in the very early Universe are generally predicted by various early cosmology scenarios [4–9]. Currently, the B-mode polarization of cosmic microwave background (CMB) radiation is a promising channel to detect PGWs [10], which may enable us to test the origin of the Universe soon.

In recent years, the secondary GWs induced by the nonlinear coupling of scalar perturbations have been attracting great attention. Those are regarded as a reasonable tool to detect a type of ultracompact objects that may exist in the early Universe—primordial black holes (PBHs) [11–22], and to probe the properties of the small-scale primordial curvature perturbations [23–35]. Overdense regions in the early Universe may stop expanding and collapse to form PBHs [36–38]. Sufficiently large density fluctuations for PBH formation can be realized in various inflationary models, e.g., the ultraslow-roll phase [39–47], the extra fields [21,48–54], the non-Gaussianity [55–60], and parametric resonance or tachyonic instability [61–67]. Those enhanced small-scale scalar perturbations also induce sizable GWs via nonlinear couplings, which can exceed the sensitivities of several upcoming GW observations, such as LISA [68], DECIGO [69], Taiji [70], and TianQin [71].

We often consider the evolution or generation of tensor fluctuations in the classical field theory with the stochastic initial conditions set by inflation. As a result, we predict the power spectrum of GWs that is related to the observables such as the CMB power spectrum or GW energy density. Previous secondary GW studies mainly focus on the autopower spectrum of second-order scalar-induced gravitational waves (SIGWs), which is a part of the classical stochastic one-loop correction to the primordial tensor-power spectrum. Subleading-order SIGWs, i.e., two-loop corrections, were also investigated in the previous literature [72–74], which should be subdominant as far as the perturbative expansion is convergent. Another possible extension at one-loop order is to include the linear vector

*iascchao@ust.hk
†iasota@ust.hk
‡hzhuav@connect.ust.hk
§yzhucc@connect.ust.hk

and tensor perturbations in the second-order source. References [75,76] considered the autospectrum of the second-order tensor modes sourced by scalar and tensor perturbations. This class of secondary GWs should also be subdominant unless the internal tensor propagator is more enhanced than the scalar propagators at some scales. So far, so good. Is there any other source of the secondary GWs?

This paper points out several missing one-loop contributions in previous considerations about SIGWs, i.e., the cross-power spectrum of the first- and third-order tensor fluctuations. The tensor fluctuation induced by the source with two scalar and one tensor perturbations is third order in cosmological perturbations, i.e., a subdominant component at the field level. However, the cross-power spectrum of the first- and third-order tensor fluctuations is also one loop, whose order in the perturbative expansion is equivalent to that of the induced power spectrum. Indeed, the iterative solutions and the higher-order interactions are consistently considered in the theory of large-scale structure, where we consider similar classical stochastic loop calculations [77]. Then, there is no reason to ignore those effects in studies of GWs. Interestingly, Ref. [73] has already included the iterative solutions for two-loop calculations of induced GWs. However, they only considered the scalar fluctuations for initial conditions, so the one-loop correction from the cross term of first- and third order was absent.

We consider all possible sources up to third order (see Table I, and also Figs. 1 and 2). We will show that the IR behavior of the new correction is very different from that of the autospectrum discussed in the previous literature and can be important for the actual gravitational wave measurements. A recent work [22] also reported the one-loop quantum corrections to PGWs by an excited spectator field, using the in-in formalism during inflation. Their consistent loop calculation showed that superhorizon PGWs are amplified or suppressed by the loop effect. Inspiringly, these astonishing results show the possibility of probing the extremely small-scale phenomena during inflation with large-scale GW observations. In this paper, we consider the classical counterpart of their scale-invariant corrections. We will show a similar effect in a classical setup in universes dominated by radiation or dust.

TABLE I. Possible source terms at third order, including tensor and scalar perturbations. The first line corresponds to the Born approximation, and the first iterative source is shown in the second to the fifth line. h and ϕ represent the tensor and scalar perturbations, respectively. ϕ implies either the curvature perturbation Ψ or gravitational potential Φ. A product of ϕ and h in a subscript implies the source of the corresponding second-order perturbations (e.g., $h_{\phi h}$ means $h^{(2)}$ sourced by $h^{(1)}\phi^{(1)}$). The underlined terms are correlated with linear tensor modes. (a) to (i) indicate the corresponding diagrams in Fig. 1 (note that Green functions are implicit).

Born approximation	$\phi\phi\phi$	$^{(d)}\underline{h\phi\phi}$	$hh\phi$	$^{(e)}\underline{hhh}$
1st iteration	$\phi h_{\phi\phi}$	$^{(b)}\underline{\phi h_{\phi h}}$	ϕh_{hh}	
	$^{(f)}\underline{h\phi_{\phi\phi}}$	$h\phi_{\phi h}$	$^{(b,h)}\underline{h\phi_{hh}}$	
	$\phi\phi_{\phi\phi}$	$^{(a)}\underline{\phi\phi_{\phi h}}$	$\phi\phi_{hh}$	
	$^{(g)}\underline{hh_{\phi\phi}}$	$hh_{\phi h}$	$^{(c,i)}\underline{hh_{hh}}$	

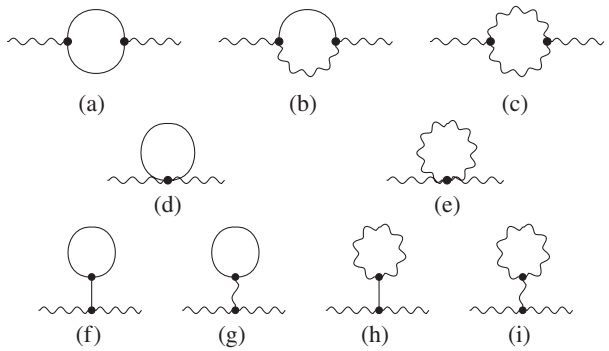

FIG. 1. Nine typical one-loop contributions to the tensor-power spectrum. The internal wavy and solid lines represent tensor and scalar propagators, respectively. The standard second-order SIGW $\mathcal{P}_h^{(22)}$ is included in diagram (a). Diagrams (b) and (c) were studied in Ref. [75], which are subdominant unless the tensor propagator is more enhanced than the scalar one. (d) is the new graph considered in this paper. We ignore (e), (h), and (i) since we only focus on the enhancement of the scalar propagator. The tadpole (g) is zero, and (f) is also negligible in the IR region. Note that we ignored vectors for simplicity.

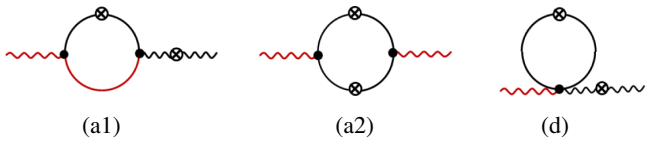

FIG. 2. Detailed structures of diagrams (a) and (d) shown in Fig. 1. We draw the diagrams following Ref. [78], while the direction of time is implicit for simplicity. The cross circle represents the contraction between two linear fields (i.e., their power spectra), which is also regarded as an "external source" in this system. The red lines are Green functions. The diagrams (a1) and (d) contribute to $\mathcal{P}^{(13)}$, while (a2) is the induced GWs $\mathcal{P}^{(22)}$.

The paper is organized as follows. In Sec. II, we extend cosmological perturbation theory to third order by including the linear tensor fluctuations to the nonlinear source. Then, we derive a generic form for the missing one-loop correction to secondary GWs, i.e., the cross-power spectrum $\mathcal{P}_h^{(13)}$. In Sec. III, we calculate $\mathcal{P}_h^{(13)}$ in the cases of both radiation-dominated (RD) and matter-dominated (MD) eras with a delta-function-like scalar source. Their IR behaviors are also investigated in detail. In Sec. IV, we elaborate on the influence on the tensor-to-scalar ratio from $\mathcal{P}_h^{(13)}$ in terms of the collaborative multifrequency GW

experiments for PBH detection. Finally, we summarize the results in Sec. V.

II. BASIC EQUATIONS AND SOURCES FOR CLASSICAL ONE-LOOP CORRECTION

In this section, we first derive the evolution equation for tensor fluctuations in the presence of two scalars and one tensor. Then, we integrate the equation of motion using the Green function method. In the standard SIGW calculation, one only expands the source to the second order in scalar perturbations, but we go beyond the expansion, including additional first-order tensor fluctuations.

First, we perturb the metric tensor around the spatially flat Friedmann-Lemaître-Robertson-Walker metric to the nonlinear order in scalar perturbations and tensor fluctuations. In the conformal Newtonian gauge, the metric takes the form of

$$ds^2 = -a^2(1+2\Phi)d\tau^2 + a^2(1-2\Psi)(\delta_{ij}+h_{ij})dx^i dx^j, \tag{1}$$

and the tensor fluctuation is expanded into

$$h_{ij} = h_{ij}^{(1)} + \frac{1}{2}h_{ij}^{(2)} + \frac{1}{6}h_{ij}^{(3)} + \cdots, \tag{2}$$

where the superscript in parentheses implies the order in cosmological perturbations, and we dropped vector perturbations for simplicity. Indeed, this paper considers a delta-function-like sharp peak for scalar initial conditions, which should not induce the second-order vector perturbations from momentum conservation. So, we ignore the vector perturbations up to second order safely [32,79]. $h_{ij}^{(1)}$ is the linear tensor mode initially set by inflation, $h_{ij}^{(2)}$ is the induced tensor mode discussed in the previous literature, and $h_{ij}^{(3)}$ is the new contribution sourced at third order in cosmological perturbations. Note that $h_{ij}^{(3)}$ from the scalar fluctuations was considered in Ref. [73] for two-loop-order autopower spectrum of $h_{ij}^{(3)}$. The transverse-traceless condition is not unique when expanding the metric tensor to nonlinear orders [80]. We impose the conditions for $h_{ij}^{(n)}$ in Eq. (1), i.e., $\partial^i h_{ij}^{(n)} = h^{(n)i}{}_i = 0$, where the Latin indices are raised and lowered by the background spatial metric δ^{ij} and δ_{ij}. The Fourier integral of the tensor perturbation is written as

$$h_{ij}^{(n)}(\tau,\boldsymbol{x}) = \int \frac{d^3k}{(2\pi)^3}\sum_{\lambda=+,\times} e_{ij}^{\lambda}(\hat{k})h_{\boldsymbol{k}}^{(n)\lambda}(\tau)e^{i\boldsymbol{k}\cdot\boldsymbol{x}}, \tag{3}$$

with two orthonormal polarization bases defined as

$$e_{ij}^{(+)}(\hat{k}) = \frac{1}{\sqrt{2}}[e_i(\hat{k})e_j(\hat{k}) - \bar{e}_i(\hat{k})\bar{e}_j(\hat{k})], \tag{4}$$

$$e_{ij}^{(\times)}(\hat{k}) = \frac{1}{\sqrt{2}}[e_i(\hat{k})\bar{e}_j(\hat{k}) + \bar{e}_i(\hat{k})e_j(\hat{k})], \tag{5}$$

where $e_i(\hat{k})$ and $\bar{e}_i(\hat{k})$ are a set of orthonormal vectors perpendicular to $\boldsymbol{k}$, and $\hat{k} \equiv \boldsymbol{k}/|\boldsymbol{k}|$. We define the dimensionless power spectrum of the tensor fluctuations as

$$\langle h_{\boldsymbol{k}}^{(n)\lambda} h_{\boldsymbol{k}'}^{(m)\lambda'}\rangle = \delta_{\lambda\lambda'}(2\pi)^3\delta^3(\boldsymbol{k}+\boldsymbol{k}')\frac{2\pi^2}{k^3}\mathcal{P}_{h,\lambda}^{(nm)}. \tag{6}$$

Hereafter, we omit the polarization index when we do not have to specify a polarization component.

We go beyond the Born approximation in this paper, so the scalar fluctuations should be included up to second order:

$$\Phi = \Phi^{(1)} + \frac{1}{2}\Phi^{(2)}, \tag{7}$$

$$\Psi = \Psi^{(1)} + \frac{1}{2}\Psi^{(2)}. \tag{8}$$

$\Phi^{(2)}$ and $\Psi^{(2)}$ are the first iterative corrections relevant to the one-loop order contribution in the end. These terms contribute to the diagrams (a), (b), (f), and (h) in Fig. 1. The same contributions were also considered in Ref. [22] in the context of the one-loop inflationary power spectrum. We assume that anisotropic stress is negligible at linear order, so the gravitational potential and curvature perturbation are equivalent. Hereafter, we denote

$$\Phi^{(1)} = \Psi^{(1)} = \phi, \tag{9}$$

for notational simplicity.

Expanding the Einstein equation and projecting it onto the polarization plane, one finds

$$h_{ij}^{(n)\prime\prime} + 2\mathcal{H}h_{ij}^{(n)\prime} - \nabla^2 h_{ij}^{(n)} = \mathcal{T}_{ij}^{lm}S_{lm}^{(n)}, \tag{10}$$

where $\mathcal{H} \equiv a'/a = aH$ is the comoving Hubble parameter, and the prime denotes the derivative with respect to the conformal time τ. $\mathcal{T}_{ij}^{lm}$ is the projection operator onto the transverse-traceless plane. In Fourier space, we recast Eq. (10) into

$$h_{\boldsymbol{k}}^{(n)\prime\prime} + 2\mathcal{H}h_{\boldsymbol{k}}^{(n)\prime} + k^2 h_{\boldsymbol{k}}^{(n)} = S_{\boldsymbol{k}}^{(n)}, \tag{11}$$

where we define

$$S_{\boldsymbol{k}}^{(n)} \equiv e^{ij}(\hat{k})S_{ij,\boldsymbol{k}}^{(n)}. \tag{12}$$

Given a source term, one can integrate Eq. (11) using the Green function:

$$h_{\boldsymbol{k}}^{(n)}(x) = \int^{x} d\tilde{x} \frac{a(\tilde{x})}{a(x)} k G_{\boldsymbol{k}}^{h}(x,\tilde{x}) \frac{S_{\boldsymbol{k}}^{(n)}(\tilde{x})}{k^2}, \tag{13}$$

where $x \equiv k\tau$. $G_{\boldsymbol{k}}^{h}$ is the Green function for tensor modes which takes the following form in the RD universe:

$$k G_{\boldsymbol{k},\mathrm{RD}}^{h}(x,\tilde{x}) = \sin(x-\tilde{x}), \tag{14}$$

where $k \equiv |\boldsymbol{k}|$. In the MD universe, we have

$$k G_{\boldsymbol{k},\mathrm{MD}}^{h}(x,\tilde{x}) = x\tilde{x}[y_1(x)j_1(\tilde{x}) - j_1(x)y_1(\tilde{x})], \tag{15}$$

where $j_1(x)$ and $y_1(x)$ are the spherical Bessel functions of the first and second kind, respectively.

Possible terms in $S_{lm}^{(3)}$ are summarized in Table I, and terms correlated with first-order tensor fluctuations are underlined. We will consider the cross-power spectrum between the first- and third-order tensor modes so we do not have to evaluate the most general forms. The operator products that appear in the final spectrum are, up to the transfer functions and Green functions, written as

$$\langle h_{\boldsymbol{k}'}^{(1)} h_{\boldsymbol{k}}^{(3)} \rangle' \sim \int \frac{d^3\mathbf{p} d^3\mathbf{q}}{(2\pi)^6} \langle h_{\boldsymbol{k}'} h_{\boldsymbol{k}-\boldsymbol{p}-\boldsymbol{q}} \phi_{\boldsymbol{p}} \phi_{\boldsymbol{q}} \rangle', \tag{16}$$

where the prime on the bracket implies that we drop a delta function with respect to the external momenta. The rhs of Eq. (16) reduces to

$$\langle h_{\boldsymbol{k}'} h_{\boldsymbol{k}} \rangle' \int \frac{d^3\mathbf{p}}{(2\pi)^3} \langle \phi_{\boldsymbol{p}} \phi_{-\boldsymbol{p}} \rangle'. \tag{17}$$

Thus, tensor fluctuation decouples from the loop, and the integral structure is simplified. Therefore, we justify the following replacement in the source:

$$\int \frac{d^3\mathbf{p} d^3\mathbf{q}}{(2\pi)^6} h_{\boldsymbol{k}-\boldsymbol{p}-\boldsymbol{q}} \phi_{\boldsymbol{p}} \phi_{\boldsymbol{q}} \to h_{\boldsymbol{k}} \int \frac{d^3\mathbf{p}}{(2\pi)^3} \phi_{\boldsymbol{p}} \phi_{-\boldsymbol{p}}. \tag{18}$$

Finally, cross-correlating the third-order tensor fluctuation with the linear one, we obtain

$$\mathcal{P}_h^{(13)}(\tau,k) = \mathcal{P}_h^{(11)}(k) \int \frac{du}{u} I_h(u,x) \mathcal{P}_\phi^{(11)}(ku), \tag{19}$$

where we use Eq. (18) and defined $u \equiv p/k$. $\mathcal{P}_h^{(11)}$ and $\mathcal{P}_\phi^{(11)}$ are the initial linear power spectra of tensor and scalar perturbations, respectively. All details about the source are included in the kernel function:

$$I_h(u,x) = T_h(x) \int^{x} d\tilde{x} \frac{a(\tilde{x})}{a(x)} k G_{\boldsymbol{k}}^{h}(x,\tilde{x}) f_h(u,\tilde{x}), \tag{20}$$

where T_h is the linear transfer function for tensor fluctuations, and $f_h(u,x)$ can be found from the concrete calculation of the source function discussed below.

A. Born approximation

The first relevant correction is the Born approximation for the third-order source. Dropping other irrelevant terms, the third-order source from the triple product of the pure first-order perturbations is given as

$$\begin{aligned} S_{h\phi\phi,ij}^{(3)} \equiv{}& h_{ij}^{(1)} \left[16\phi\nabla^2\phi + \frac{8(1+3\omega)}{3(1+\omega)} (\nabla\phi)^2 - \frac{32\nabla\phi\nabla\phi'}{3\mathcal{H}(1+\omega)} - \frac{16(\nabla\phi')^2}{3\mathcal{H}^2(1+\omega)} \right] - 24\phi(3\phi' h_{ij}^{(1)\prime} + 2\phi\nabla^2 h_{ij}^{(1)}) \\ & - \frac{16\partial^k\phi}{\mathcal{H}^2(1+\omega)} \left[(\mathcal{H}\partial_j\phi + \partial_j\phi') h_{ki}^{(1)\prime} + (\mathcal{H}\partial_i\phi + \partial_i\phi') h_{kj}^{(1)\prime} \right] + 24\phi\partial^k\phi(\partial_j h_{ki}^{(1)} + \partial_i h_{kj}^{(1)} - \partial_k h_{ij}^{(1)}), \end{aligned} \tag{21}$$

where we simplified the source, using the equations of motion for ϕ and $h_{ij}^{(1)}$. Under the premise of Eq. (18), we find

$$\begin{aligned} S_{h\phi\phi,\boldsymbol{k}}^{(3)} = -\int \frac{d^3\mathbf{p}}{(2\pi)^3} \Bigg[& \frac{8(5+3\omega)}{3(1+\omega)} p^2 h_{\boldsymbol{k}} \phi_{\boldsymbol{p}} \phi_{-\boldsymbol{p}} + \frac{32}{3(1+\omega)\mathcal{H}} p^2 (h_{\boldsymbol{k}} \phi_{\boldsymbol{p}}' \phi_{-\boldsymbol{p}} + h_{\boldsymbol{k}}' \phi_{\boldsymbol{p}} \phi_{-\boldsymbol{p}}) \\ & + \frac{16}{3(1+\omega)\mathcal{H}^2} p^2 (h_{\boldsymbol{k}} \phi_{\boldsymbol{p}}' \phi_{-\boldsymbol{p}}' + 2h_{\boldsymbol{k}}' \phi_{\boldsymbol{p}}' \phi_{-\boldsymbol{p}}) + 72 h_{\boldsymbol{k}}' \phi_{\boldsymbol{p}}' \phi_{-\boldsymbol{p}} - 48k^2 h_{\boldsymbol{k}} \phi_{\boldsymbol{p}} \phi_{-\boldsymbol{p}} \Bigg]. \end{aligned} \tag{22}$$

Then, we get

$$f_{h,h\phi\phi}(u,x) \equiv -\Big\{\frac{8(5+3\omega)}{3(1+\omega)}u^2T_h(x)T_\phi(ux)T_\phi(ux)+\frac{8(1+3\omega)^2}{3(1+\omega)}u^2x^2T_h'(x)T_\phi'(ux)T_\phi(ux)$$
$$-48T_h(x)T_\phi(ux)T_\phi(ux)+72T_h'(x)T_\phi'(ux)T_\phi(ux)+\frac{4(1+3\omega)^2}{3(1+\omega)}u^2x^2T_h(x)T_\phi'(ux)T_\phi'(ux)$$
$$+\frac{16(1+3\omega)}{3(1+\omega)}u^2x[T_h(x)T_\phi'(ux)T_\phi(ux)+T_h'(x)T_\phi(ux)T_\phi(ux)]\Big\}, \tag{23}$$

where we used the conformal Hubble parameter, written as

$$\mathcal{H}=\frac{2}{(1+3\omega)\tau}. \tag{24}$$

Note that the prime denotes the derivative with respect to x hereafter. T_h and T_ϕ are transfer functions for the linear tensor and scalar modes, respectively. Following the similar treatments in Refs. [15,81], one can find the analytical solution of the kernel function $I_{h,h\phi\phi}(u,x)$.

B. First iterative solution

In addition to the Born approximation, we need to account for the first iterative solution for the one-loop-order correction to the cross-power spectrum. We summarized possible sources in Table I, but it is found that only $\phi\phi_{\phi h}$ is the relevant contribution in our case. $\phi h_{\phi h}$, $hh_{\phi\phi}$, and $h\phi_{\phi\phi}$ are potentially comparable to $\phi\phi_{\phi h}$. However, these terms contribute in the subhorizon region where the induced GWs dominate, as discussed in Appendix A. As discussed in the next section, we may ignore those contributions when we are interested in the IR region. We also safely ignore hhh, hh_{hh}, $h\phi_{hh}$ since they are not amplified by scalar fluctuations.

The source terms from ϕ and second-order scalar induced by ϕ and h are written as

$$S^{(3)}_{\phi\phi_{\phi h},ij}=\frac{8}{\mathcal{H}^2(1+\omega)}[(\mathcal{H}\partial_i\phi+\partial_i\phi')(\mathcal{H}\partial_j\Phi^{(2)}+\partial_j\Psi^{(2)\prime})$$
$$+(i\leftrightarrow j)]-12[(\Phi^{(2)}+\Psi^{(2)})\partial_i\partial_j\phi$$
$$+\phi\partial_i\partial_j(\Phi^{(2)}+\Psi^{(2)})+\partial_i\phi\partial_j\Psi^{(2)}+\partial_j\phi\partial_i\Psi^{(2)}]. \tag{25}$$

The difference of $\Phi^{(2)}$ and $\Psi^{(2)}$ arises from $\mathcal{O}(\phi^2,\phi\partial h)$. Hence, we can take $\Phi^{(2)}=\Psi^{(2)}$ and drop derivative terms like ∂h in the following calculation for the IR region. The equation of motion for $\Psi^{(2)}$ is given as

$$\Psi^{(2)\prime\prime}+3\mathcal{H}(1+\omega)\Psi^{(2)\prime}-\omega\nabla^2\Psi^{(2)}=-2\omega h^{(1)}_{ij}\partial_i\partial_j\phi. \tag{26}$$

We immediately find $\Psi^{(2)}=0$ for the matter era where $\omega=0$. During the radiation era, we get [19]

$$\Psi^{(2)}_{\boldsymbol{k}+\boldsymbol{p}}(\tau)=\frac{1}{\sqrt{2}}\sin^2\theta\cos 2\varphi I_{\phi,\mathrm{RD}}(u,v,x)\phi^0_{\boldsymbol{p}}h^0_{\boldsymbol{k}}, \tag{27}$$

where h^0_k and ϕ^0_p are the initial value at the superhorizon scale, and

$$I_{\phi,\mathrm{RD}}(u,v,x)=\int^x d\tilde{x}\frac{\tilde{x}^2}{x^2}kG^s_{\boldsymbol{k}}(vx,v\tilde{x})\frac{u^2}{v}\frac{2}{3}T_h(\tilde{x})T_\phi(u\tilde{x}). \tag{28}$$

Note that we defined $v\equiv|\boldsymbol{p}+\boldsymbol{k}|/k$, and (θ,φ) are the spherical coordinates of $\boldsymbol{p}$ with respect to $\hat{z}\|\boldsymbol{k}$, and the Green function for scalar perturbations is

$$kG^s_{\boldsymbol{k}}(x,\tilde{x})=\frac{x\tilde{x}}{\sqrt{3}}\left[j_1\left(\frac{\tilde{x}}{\sqrt{3}}\right)y_1\left(\frac{x}{\sqrt{3}}\right)-(x\leftrightarrow\tilde{x})\right]. \tag{29}$$

Substituting Eq. (27) into Eq. (25), we find the first iterative solution. The rest of the calculation is the same as the Born approximation, so we find

$$f_{h,\phi\phi_{\phi h}}(u,v,x)=\int d\theta\sin^5\theta\frac{3}{2}u^2\times\Big[3T_\phi I_{\phi,\mathrm{RD}}$$
$$+x(T_\phi' I_{\phi,\mathrm{RD}}+T_\phi I'_{\phi,\mathrm{RD}})+x^2T_\phi' I'_{\phi,\mathrm{RD}}\Big]. \tag{30}$$

III. IR BEHAVIOR OF THE ONE-LOOP CORRECTION

In the previous section, we obtained the new one-loop contribution:

$$\mathcal{P}^{(13)}_h(\tau,k)=\mathcal{P}^{(11)}_h(k)\int\frac{du}{u}(I_{h,h\phi\phi}+I_{h,\phi\phi_{\phi h}})\mathcal{P}^{(11)}_\phi(ku), \tag{31}$$

where the kernels $I_{h,h\phi\phi}$ and $I_{h,\phi\phi_{\phi h}}$ are defined through Eq. (20), with the source integrals $f_{h,h\phi\phi}$ and $f_{h,\phi\phi_{\phi h}}$ given by Eqs. (23) and (30), respectively.

Equation (31) implies that the new one-loop contributions are roughly written as $\mathcal{P}_h^{(13)} \sim \mathcal{P}_h^{(11)}\mathcal{P}_\phi^{(11)}$. In comparison, the SIGW autopower spectrum is $\mathcal{P}_h^{(22)} \sim (\mathcal{P}_\phi^{(11)})^2$. Therefore, one may naively expect that the new contributions are suppressed by a factor of $\mathcal{P}_h^{(13)}/\mathcal{P}_h^{(22)} \sim \mathcal{P}_h^{(11)}/\mathcal{P}_\phi^{(11)}$, which should be the subdominant of secondary GWs. Is that true? Equation (18) suggests that the new third-order correction is not a production of GWs from zero but a modulation of primordial tensor fluctuations due to couplings between tensor and scalar. The physical origin differs from the GW production, so the property is not necessarily the same. Indeed, we will show that the new contribution can be dominant in the IR region.

In this section, we concretely compute $\mathcal{P}_h^{(13)}$ for a simple but phenomenologically interesting delta-function-like scalar power spectrum. We often consider the delta-function-like spectrum for the SIGW counterpart of PBH formation scenarios, and the SIGWs from the source have peaks near the sharp peak of scalar fluctuations. In the IR region, $\mathcal{P}_h^{(22)}$ is suppressed as SIGWs are causally generated from physical processes. Here, we will show that the IR behavior of the new correction is very different from that of the autopower spectrum of the SIGWs [82], and $\mathcal{P}_h^{(13)}$ can be dominant for large-scale tensor fluctuations. In the following, we consider universes dominated by radiation and dust separately and compare their behaviors with the standard SIGWs.

A. Radiation-dominated era

During the RD era, $\omega = 1/3$, and the transfer functions are given as

$$T_\phi(x) = \frac{9}{x^2}\left[\frac{\sin(x/\sqrt{3})}{x/\sqrt{3}} - \cos\left(\frac{x}{\sqrt{3}}\right)\right], \tag{32}$$

$$T_h(x) = j_0(x) = \frac{\sin x}{x}. \tag{33}$$

The source functions are the sum of

$$f_{h,h\phi\phi} = T_h[(48-12u^2)T_\phi T_\phi - 8u^2 x T'_\phi T_\phi - 4u^2x^2T'_\phi T'_\phi] - T'_h(8u^2x^2T'_\phi T_\phi + 8u^2xT_\phi T_\phi + 72T'_\phi T_\phi), \tag{34}$$

$$f_{h,\phi\phi_{\phi h}} = \int d\theta \sin^5\theta \frac{3}{2}u^2 \times [3T_\phi I_{\phi,\mathrm{RD}} + x(T'_\phi I_{\phi,\mathrm{RD}} + T_\phi I'_{\phi,\mathrm{RD}}) + x^2 T'_\phi I'_{\phi,\mathrm{RD}}], \tag{35}$$

where the arguments are suppressed for notational simplicity, while T_ϕ and T_h are functions of ux and x, respectively. We consider the delta-function-like source amplified at $k = k_*$, i.e.,

$$\mathcal{P}_\zeta^\delta(k) = A_\zeta \delta(\ln k - \ln k_*), \tag{36}$$

where A_ζ is the overall amplitude. The relationship between the superhorizon comoving curvature perturbation ζ and Newtonian potential ϕ is

$$\phi_{\boldsymbol{k}} = \frac{3+3\omega}{5+3\omega}\zeta_{\boldsymbol{k}}. \tag{37}$$

Combining Eqs. (19), (20), and (32) to (37), we reach the final result of $\mathcal{P}_h^{(13)}(k,\tau)$. Equation (35) contains two layers of Green function integrals, whose analytical result is tedious. However, we can simplify the expressions in the IR region since the solution of Eq. (26) is written as $\Psi_{\boldsymbol{p}}^{(2)}(\tau) \sim \tau\phi'_{\boldsymbol{p}}(\tau)$ for the superhorizon tensor modes.

The final expression has a factorized form:

$$\frac{1}{6}\mathcal{P}_h^{(13)}(k,\tau) \equiv \mathcal{F}(k_*,k,\tau)\mathcal{P}_h^{(11)}(k), \tag{38}$$

where the prefactor $\mathcal{F}$ for $k\tau < 1$ scales as

$$\mathcal{F}(k_*,k,\tau)|_{k\tau<1} \simeq A_\zeta\left[2 - 2.4\log(k_*\tau) + \mathcal{O}\left(\frac{k}{k_*}\right)\right]. \tag{39}$$

Thus, $\mathcal{F}$ is k independent for $k/k_* \ll 1$ modes, and the one-loop correction $\mathcal{P}_h^{(13)}$ has the same scaling as the linear power spectrum $\mathcal{P}_h^{(11)}$ on the superhorizon scales. The above scale dependence arises from Eq. (34) and Eq. (35), but their signs are opposite. They are partly canceled by each other, and the total contribution is dominated by Eq. (34). As a result, the new one-loop order correction decreases the primordial spectrum. We show the analytical expression from the dominated source $h\phi\phi$ in Appendix B. Since $\mathcal{F}$ is linear with respect to $\mathcal{P}_\zeta^\delta$, we can straightforwardly generalize Eq. (39) for an arbitrary scalar spectrum. As we have

$$\mathcal{P}_\zeta(k) = \int d\,\ln k_* \mathcal{P}_\zeta(k_*)\delta(\ln k - \ln k_*), \tag{40}$$

we find

$$\mathcal{F}(k,\tau) = \frac{1}{A_\zeta}\int d\,\ln k_* \mathcal{P}_\zeta(k_*)\mathcal{F}(k_*,k,\tau). \tag{41}$$

The τ dependence of Eq. (39) implies that the scalar peak at $k = k_*$ contributes to $\mathcal{P}_h^{(13)}$ at any time after the horizon

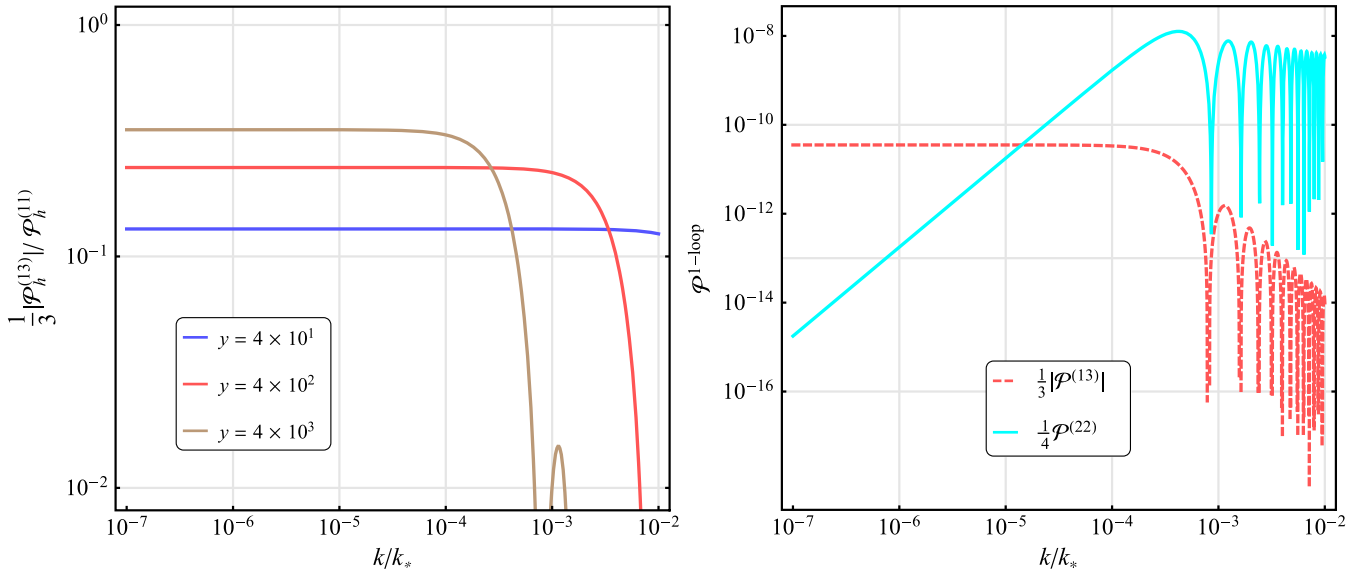

FIG. 3. Left: the absolute value of the one-loop correction $\frac{1}{3}|\mathcal{P}_h^{(13)}|$ shown in Eq. (31) as a function of k/k_* during the RD era. The vertical axis is normalized by the primordial tensor spectrum $\mathcal{P}_h^{(11)}$. Brown, red, and blue solid lines denote different times: $y \equiv k_*\tau = 4\times10^1, 4\times10^2$, and 4×10^3, respectively. The damping feature for $k/k_* \gtrsim y^{-1}$ implies the horizon entry. Right: a comparison between the amplitudes of the one-loop corrections $|\mathcal{P}_h^{(13)}|$ and the standard second-order SIGWs $\mathcal{P}_h^{(22)}$ during the RD era, which are shown by the red dashed and the cyan solid curves, respectively. The parameters are taken as $y_{\rm D} = 4\times10^3$, $A_\zeta = 10^{-2}$, and $\mathcal{P}_h^{(11)} = 10^{-10}$.

reentry of the scalar peak. This is because we ignored the shear viscosity in the radiation fluid for simplicity. With this approximation, sound waves propagate forever. In the real Universe, photons are coupled to electrons via Compton scattering, which introduces acoustic dissipation. Then, the inhomogeneity inside the diffusion scale is smeared. As a result, the gravitational potential and curvature perturbations are erased. The photon-diffusion scale is given by [83]

$$k_{\rm D} \sim 2.34\times10^{-5}\Theta_{2.7}(1-Y_{\rm p}/2)^{1/2}\Omega_b^{1/2}z^{3/2}\,h/{\rm Mpc} \sim 4.9\times10^{-6}z^{3/2}\,h/{\rm Mpc}, \tag{42}$$

with a normalized CMB temperature $\Theta_{2.7} = T_{\rm CMB}/2.7 = 1.01$, the primordial helium mass fraction $Y_{\rm p} = 0.23$, and the baryon energy-density fraction $\Omega_{\rm b} = 0.0486$. Then, the scalar fluctuations with $k > k_{\rm D}$ are exponentially suppressed because of the diffusion effect. Solving $k_* = k_{\rm D}(z(\tau_{\rm D}))$ for $\tau_{\rm D}$, we find the final amplitude at $\tau = \tau_{\rm D}$, that is, $\mathcal{F}(k_*, k, \tau_{\rm D})$. The source vanishes for $\tau > \tau_{\rm D}$, so the superhorizon tensor fluctuations should not vary anymore. Since the loop momentum in Eq. (19) is independent of the external momentum k, momentum conservation does not introduce any additional factor. In contrast, the Heaviside step function appears due to momentum conservation in $\mathcal{P}_h^{(22)}$ [15,81].

Let us consider a specific case with $k_* \sim 10^5\,h/{\rm Mpc}$ as a reference scale for PBH formation during the RD era, corresponding to tens of solar masses which may account for LIGO/Virgo GW detection events [84,85]. The conformal time when $k_* \sim 10^5\,h/{\rm Mpc}$ enters the diffusion scale is estimated to be $\tau_{\rm D} \sim 0.04\ {\rm Mpc}/h$. Then we find $y_{\rm D} \equiv k_*\tau_{\rm D} \sim 4\times10^3$. In the left panel of Fig. 3, we plot $|\mathcal{P}_h^{(13)}|/3$, where the coefficient $1/6$ comes from the metric decomposition (1) and a factor of 2 appears in the cross term. Brown, red, and blue solid lines in the left panel of Fig. 3 denote different times $y(\equiv k_*\tau) = 4\times10^1, 4\times10^2$, and 4×10^3, respectively, and we normalize the total power spectrum by the linear power spectrum $\mathcal{P}_h^{(11)}$. We find that the one-loop correction $\mathcal{P}_h^{(13)}$ results in a *negative constant* on the superhorizon scales, which suppresses the scale-invariant primordial tensor-power spectrum. With observationally allowable curvature perturbations [27,86] (also see Fig. 5), $A_\zeta < 10^{-2}$ at $k_* \sim 10^5\,h\,{\rm Mpc}^{-1}$, we find that the initial tensor-power spectrum loses the amplitude by at most 35%. After the horizon reentry, the tensor modes evolve as if they are the linear tensor modes described by the red dashed curve in the right panel of Fig. 3. We emphasize that $\mathcal{P}_h^{(13)}$ displays a distinct IR behavior from that of $\mathcal{P}_h^{(22)}$ due to the decoupling of the first-order tensor and scalar fluctuations in Eq. (18). The universal IR scaling of secondary GWs discussed in Ref. [82] applies to a bilinear source, which does not lead to such a decoupling in our paper.

As discussed in Ref. [22], the suppression of the primordial tensor mode may result from the effective mass

of the tensor fluctuation introduced by the one-loop correction in the effective action. When integrating out the scalar perturbations, we may write the equation of motion of the tensor fluctuations as follows:

$$h_{\boldsymbol{k}}''(\tau) + 2\mathcal{H}h_{\boldsymbol{k}}'(\tau) + (k^2 + m_{\rm eff}^2)h_{\boldsymbol{k}}(\tau) = 0, \tag{43}$$

and $m_{\rm eff}^2$ is found to be positive in our case. This mass term introduces a decaying solution even for $k\tau \ll 1$, as far as $\tau^2 m_{\rm eff}^2 \gtrsim 1$. The evolution of superhorizon tensor fluctuations in the separate Universe perspective is also discussed in Ref. [87]. We also show the comparison of our new result $|\mathcal{P}_h^{(13)}|/3$ and the standard second-order SIGWs $\mathcal{P}_h^{(22)}$ in the right panel of Fig. 3. Here, the dimensionless time variable $y_{\rm D}$ is taken as 4×10^3, and the amplitudes of the scalar and the primordial tensor spectra are chosen as $A_\zeta = 10^{-2}$ and $\mathcal{P}_h^{(11)} = 10^{-10}$, respectively. $\mathcal{P}_h^{(13)}$ overwhelms $\mathcal{P}_h^{(22)}$ in the IR region, so the one-loop correction to the tensor spectrum on the superhorizon scale is dominated by $\mathcal{P}_h^{(13)}$.

B. Early matter-dominated era

After inflation, the oscillation of massive fields effectively acts as pressureless dust. Hence, there may be an early MD period. The second-order SIGWs $\mathcal{P}_h^{(22)}$ during this era have been studied in Refs. [12,15,75,88–92]. Since the gravitational potential is constant during the MD era, sizable SIGWs may be produced during the early MD era. Therefore, we also investigate our new effect during the early MD era in this section. The transfer functions during the MD era are given as

$$T_\phi(x) = 1, \tag{44}$$

$$T_h(x) = \frac{3j_1(x)}{x}. \tag{45}$$

Thus, the linear gravitational potential is constant during the MD era, and the source function in Eq. (23) is greatly simplified as

$$\begin{aligned} f_{h\phi\phi}(u,x) &= T_\phi T_\phi\left(-\frac{40}{3}u^2 T_h + 48T_h - \frac{16}{3}u^2 x T_h'\right) \\ &= \frac{8[18 + u^2(1-2x^2)]}{x^3}\sin x - \frac{8(u^2+18)}{x^2}\cos x, \end{aligned} \tag{46}$$

and the iterative part is zero from Eq. (26). Combining Eqs. (46) with (19), we find the one-loop correction,

$$\begin{aligned} \frac{\mathcal{P}_h^{(13)}(\tau,k)}{\mathcal{P}_h^{(11)}} = \int \frac{dp}{p} &\frac{12(k\tau\cos k\tau - \sin k\tau)}{(k\tau)^6} \\ &\times [k\tau(54 - p^2\tau^2)\cos k\tau \\ &+ (p^2\tau^2 + 18k^2\tau^2 - 54)\sin k\tau] \\ &\times \left(\frac{3}{5}\right)^2 \mathcal{P}_\zeta(p). \end{aligned} \tag{47}$$

Let us consider a delta-function-like source in Eq. (36). The final expression is similar to Eq. (38), while the prefactor $\mathcal{F}$ is given as

$$\mathcal{F}(k_*,k,\tau)|_{k\tau<1} \simeq -\frac{2}{25}A_\zeta k_*^2\tau^2. \tag{48}$$

We show the power spectrum of the tensor modes in Fig. 4 for $A_\zeta = 10^{-4}$. The primordial power spectrum normalizes the final result. In the left panel, from top to bottom, brown, red, and solid blue lines denote different times $y = 10^2, 10^3$, and 10^4, respectively. Since the scalar source is constant after horizon entry, it can continuously generate the tensor modes. In the right panel of Fig. 4, we compare $|\mathcal{P}^{(13)}|$ and $\mathcal{P}^{(22)}$. Here, we take $y = 10^2$, the amplitude is $A_\zeta = 10^{-4}$, and $\mathcal{P}_h^{(11)} = 10^{-10}$.

Large enhancement of second-order SIGWs was also discussed in the previous literature, but there is a caveat about the induced tensor modes during the matter era. Induced tensor modes contain not only the GWs, but also nonpropagating modes during the matter era, and the latter is mainly amplified. We cannot regard the nonpropagating component as GWs since its energy contribution to the cosmic expansion is a^{-2}, i.e., the nonpropagating part represents the curvature rather than the GWs. References [90,91] showed that the curvature is converted into the GWs if the transition from matter to radiation is faster than the oscillation timescale of scalar perturbations, and the curvature dilutes without sourcing the GWs if the transition is slow. The same argument may apply to the present case, i.e., the final amplitude may be sensitive to the transition between two eras. We leave further investigation for future work.

C. Late matter-dominated era

The early-matter dominance is hypothetical, but late-time matter dominance from recombination to dark-energy dominance is manifest. We have already observed tiny and almost scale-invariant scalar fluctuations at that scale. Does the observed curvature fluctuation change the CMB B-mode during the late-time matter era? The subhorizon gravitational potential damps during the radiation era, so there is a natural UV cutoff in the loop integral. For simplicity, let us assume

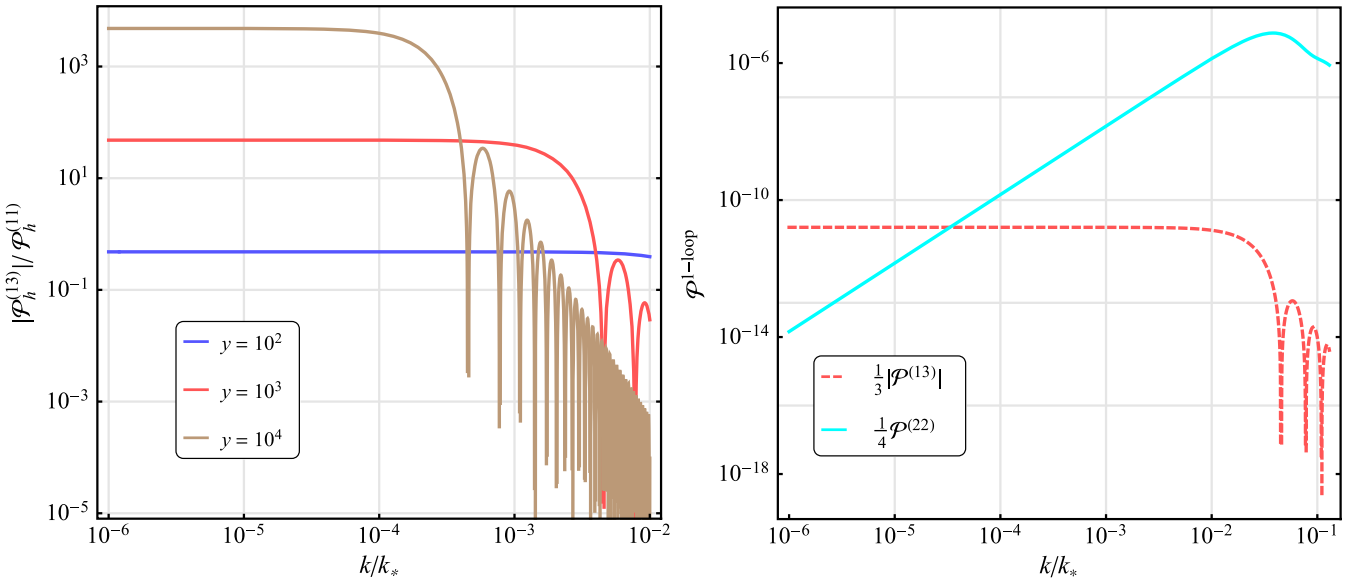

FIG. 4. Left: absolute value of the one-loop correction $|\mathcal{P}_h^{(13)}|$ sourced by the delta-function-like source during MD era. The vertical axis is normalized by the primordial tensor spectrum $\mathcal{P}_h^{(11)}$, and A_ζ is taken to be 10^{-4}. Brown, red, and blue solid lines denote different times: $y \equiv k_*\tau = 10^2, 10^3$, and 10^4, respectively. The damping feature for $k/k_* \gtrsim y^{-1}$ implies the horizon entry. Right: comparison between two types of one-loop SIGWs power spectra. The cyan curve refers to $\frac{1}{4}\mathcal{P}_h^{(22)}$ while the red dashed line represents $\frac{1}{3}|\mathcal{P}_h^{(13)}|$. Here, the dimensionless time y is chosen to be 10^2, $A_\zeta = 10^{-4}$, and $\mathcal{P}_h = 10^{-10}$.

$$\mathcal{P}_\zeta^c = A_\zeta \Theta(k_{\rm eq} - k), \tag{49}$$

where Θ is the Heaviside step function, $A_\zeta \sim 2.1 \times 10^{-9}$, and $k_{\rm eq} \sim 0.01\ h/\text{Mpc}$ is the horizon scale of the matter-radiation equality. In this case, using Eq. (41), the super-horizon spectrum is suppressed by a factor of

$$\mathcal{F}(k,\tau) \sim -\frac{1}{25} A_\zeta (k_{\rm eq}\tau)^2. \tag{50}$$

At recombination time $\tau_{\rm rec} \sim 300\ \text{Mpc}/h$, $k_{\rm eq}\tau_{\rm rec} = \mathcal{O}(1)$, so the correction is tiny, that is, $\mathcal{P}_h^{(13)}/\mathcal{P}_h^{(11)} = \mathcal{O}(A_\zeta)$. Therefore, the CMB polarization from recombination will remain unchanged. Reionization also introduces low-ℓB modes with less lensing contamination. The reionization time is given as $\tau_{\rm reio} \sim 4000\,\text{Mpc}/h$, so we find $\mathcal{P}_h^{(13)}/\mathcal{P}_h^{(11)} = \mathcal{O}(10^3 A_\zeta)$, which could also be too small for the experiments. Therefore, we conclude that we will not see a reduction in the CMB polarization in the present case. However, we only consider the linear evolution of the scalar fluctuation in the late-matter era. The nonlinear evolution of cosmological perturbations plays an essential role during the matter era. Hence, including enhancement due to the nonlinearity in the above estimation will be interesting.

IV. COLLABORATIVE MULTIFREQUENCY GW EXPERIMENTS FOR PBH DETECTION

The direct measurement of stochastic GW background may tell us the amplitude of the small-scale curvature perturbations A_ζ and the mass distribution of PBHs in future observations. Then, we point out that low-frequency GWs may be secondarily reduced by large A_ζ, which could be tested in the next-generation CMB experiments. For example, CMB-S4 and LiteBIRD, next-generation ground-based and space-based experiments, are expected to reach an upper limit of $r < 0.001$ [10,93]. Thus, combining the multifrequency GW experiments range from 10^{-15} to 10^4 Hz, from CMB polarization to the LIGO/Virgo, should be crucial to discuss PBH formation theories.

The accumulated effect of the one-loop correction $\mathcal{P}_h^{(13)}$ from the RD era ceases at $\tau_{\rm D}$ since scalar fluctuations below the diffusion scale $k_{\rm D}$ are exponentially suppressed as discussed in Sec. III A. The one-loop calculation during the MD era requires further investigation of nonlinear dynamics, so we limit our quantitative arguments to the RD era. In our case, the tensor-to-scalar ratio on the CMB scale is written as

$$r \equiv \frac{2\left(\frac{1}{3}\mathcal{P}_h^{(13)}(\tau_{\rm D}) + \mathcal{P}_h^{(11)}\right)}{A_\zeta^{\rm CMB}} = r^{(11)}(1 + \Delta_r), \tag{51}$$

where $\mathcal{P}_h^{(13)}$ can be calculated in Eq. (38) and $A_\zeta^{\rm CMB} \simeq 2.1 \times 10^{-9}$ [94]. The factor 2 accounts for two polarizations

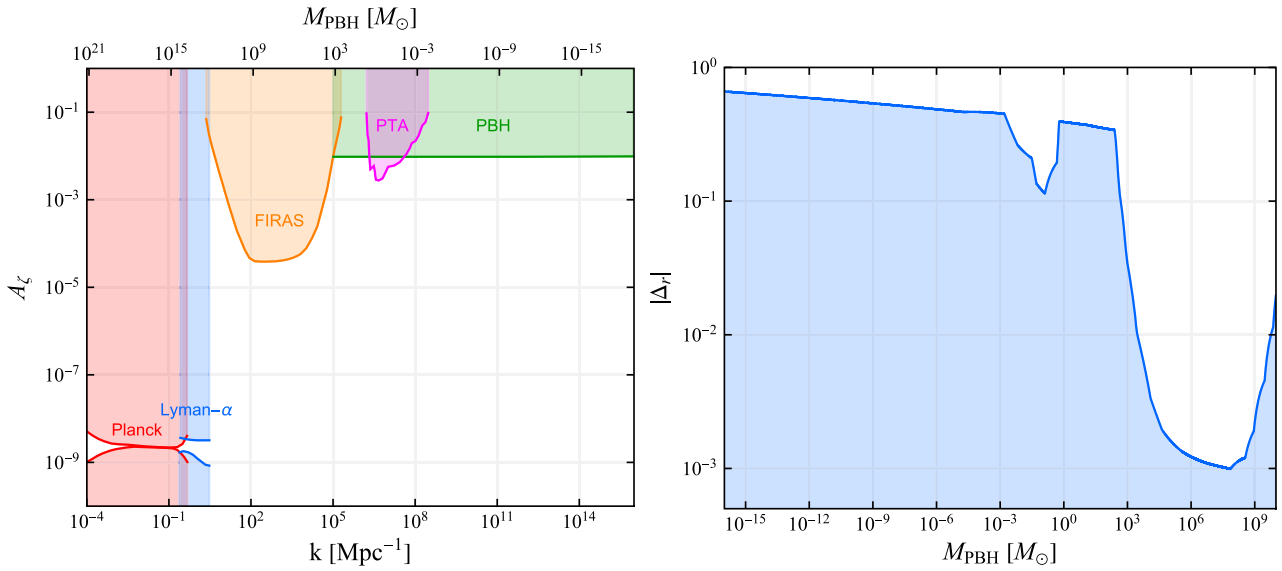

FIG. 5. Left: current constraints on the curvature perturbations on different scales, including the Planck [94] (red), Lyman-α forest [97] (blue), far infrared absolute spectrophotometer (FIRAS) CMB spectral distortion [98] (orange), and pulsar timing arrays (PTA) constraint on the standard SIGW $\mathcal{P}_h^{(22)}$ [41] (magenta). We also present constraint from PBH abundance account for dark matter [27,86] (green) with a conservative value $A_\zeta = 10^{-2}$. Similar plots can also be found in Refs. [27,41,86]. The lower horizontal axis corresponds to the peak scale k_* for the delta-function-like source. Right: upper limit on tensor-to-scalar ratio variation $|\Delta_r|$ in terms of the monochromatic PBH mass $M_{\rm PBH}$. The shadow refers to the parameter space allowed by the left panel.

of tensor modes. Note that r is evaluated at the pivot scale $k_s = 0.05\,\mathrm{Mpc}^{-1}$ for CMB observation. $r^{(11)} \equiv 2\mathcal{P}_h^{(11)}/A_\zeta^{\rm CMB}$ is the commonly used definition of the tensor-to-scalar ratio for PGWs, and it is straightforward to see that

$$\Delta_r = \frac{1}{3}\frac{\mathcal{P}_h^{(13)}(\tau_{\rm D})}{\mathcal{P}_h^{(11)}} \simeq A_\zeta[4 - 4.8\log(k_*\tau)], \tag{52}$$

which is calculated by Eq. (39). From the above expression, Δ_r depends on k_* and A_ζ. At present, A_ζ is loosely constrained as shown in the left panel of Fig. 5. However, we expect that PIXIE-like spectral distortion experiments [95] and GW experiments including SKA, LIGO, and BBO [27,95], will significantly improve the upper bounds (see Fig. 1 in Ref. [86] or Fig. 4 in Ref. [27] for details). Also, one can relate the peak scale k_* to the formation masses of PBHs by using the horizon-mass approximation [96],

$$M_{\rm PBH} \simeq \gamma M_H \simeq M_\odot\left(\frac{\gamma}{0.2}\right)\left(\frac{g_{\rm form}}{10.75}\right)^{-\frac{1}{6}}\left(\frac{k_*}{1.9\times 10^6\ \mathrm{Mpc}^{-1}}\right)^{-2}, \tag{53}$$

where $\gamma \simeq 0.2$, $g_{\rm form} \simeq 106.75$, and $M_\odot$ is the solar mass. Hence, with the constraints on A_ζ shown in the left plot in Fig. 5, we can obtain upper limits on $|\Delta_r|$ for each PBH mass $M_{\rm PBH}$.

The plot shows that the lighter PBHs reduce PGW more. Two concaves are due to the present constraints on A_ζ from FIRAS and PTA in the left panel in Fig. 5. $|\Delta_r|$ in Fig. 5 may exceed the unity for a certain small $M_{\rm PBH}$, implying the ignorance of the higher-order nonlinear terms or that we cannot trust perturbative analysis anymore because the autotensor spectrum including all corrections must be non-negative.

A remaining issue is gauge dependence. Tensor fluctuations at nonlinear order are generally gauge dependent; therefore, comparing theory and observations is not straightforward. Several works suggested that the induced GWs are physically well defined only in the subhorizon scale, and the induced GWs are gauge independent in that limit [99–102]. However, the loop effect we discussed is manifest at the superhorizon scale; that is, we consider the nonlinearity in the superhorizon tensor modes. We cannot distinguish the third-order tensor fluctuations from the linear ones once the source disappears, and the evolution afterward is linear. Therefore, the same solution does not apply to the gauge issue of the superhorizon corrections. However, as we work in the same gauge condition for the rest of cosmic history, observational predictions such as the CMB polarization should be consistent. We will further investigate the gauge dependence of the loop effect in future work.

V. CONCLUSIONS

The nonlinear interaction of cosmological perturbations secondarily induces tensor fluctuations or GWs. Such

secondary GWs are attracting growing attention as we indirectly test the PBH formation theories via future GW measurements. Recent works mostly considered the one-loop autopower spectrum of second-order induced tensor modes. This paper identified a missing one-loop contribution from the cross-power spectrum of first- and third-order tensor modes. We computed the third-order tensor fluctuation sourced by a tensor and two scalar perturbations, including higher-order nonlinear interactions and iterative solutions. Assuming a primordial tensor mode and enhanced delta-function-like scalar fluctuation in a typical PBH formation scenario, we found that the new one-loop correction is *scale invariant* and *negative* in the superhorizon region. Hence, short-scale large scalar fluctuations may significantly reduce the superhorizon primordial tensor-power spectrum. Suppose that the recent LIGO/Virgo events are explained by tens-solar-mass PBHs generated by a sharp peak of scalar fluctuations with $A_\zeta \sim 10^{-2}$ at $k_* \sim 10^5\, h/\mathrm{Mpc}$, we showed that the tensor-power spectrum at the CMB scale reduces by at most 35%. Hence, the polarization B mode might not be observed because the secondary effect of PBH formation reduced the original tensor spectrum. In a hypothetical early MD era, the reduction effect is more sensitive to the scalar amplitude since the gravitational potential is constant, implying that the loop expansion may easily fail. Hence, a detailed loop analysis will be required for further quantitative predictions in MD eras.

The new IR behavior greatly differs from the case of the second-order tensor autopower spectrum since the causally generated second-order tensor fluctuations are never correlated over the superhorizon scale. Then, does the scale-invariant reduction violate causality? The new third-order correction is not a production of GWs from zero but a shift of the existing linear tensor modes via the Fourier mode coupling at nonlinear orders. Equation (18) implies that the third-order correction is the amplitude modulation of superhorizon first-order tensor fluctuations by the subhorizon scalar fluctuations as illustrated in Fig. 6. References [103–106] discussed similar effects for CMB spectral distortion anisotropies in the presence of primordial non-Gaussianity. They found that the local non-Gaussinaity introduces the Fourier mode coupling between super- and subhorizon modes at third order. Then, the secondarily generated spectral distortions are correlated over the superhorizon scale without violating causality. The superhorizon evolution of other cosmological perturbations due to the primordial non-Gaussianity is also discussed in Refs. [32,107,108]. Our mechanism is essentially the same as this, while non-Gaussianity is naturally introduced by nonlinearity in the Einstein equation. The variation of the superhorizon tensor mode is also discussed with the separate Universe formalism in Ref. [87]. Similar IR dependence was also found in the general relativistic correction of the matter power spectrum in Ref. [109] in the context of large-scale-structure, while the correction is tiny for $\zeta \sim 10^{-5}$ in that work.

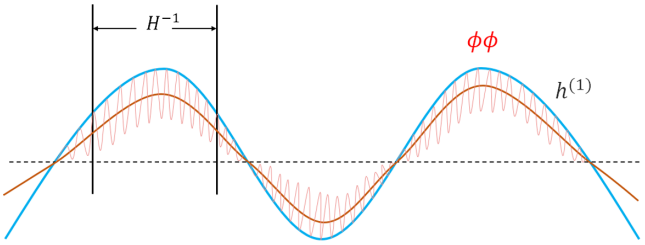

FIG. 6. Modulation of the superhorizon tensor fluctuation is illustrated. The blue sine curve means the tensor fluctuations whose wavelength is larger than the Hubble scale H^{-1}. The thin orange curve means the amplitude modulation introduced by the subhorizon scalar fluctuations coupled to the first-order tensor fluctuations. When integrating out the subhorizon scalar fluctuations, we obtain the reduced tensor fluctuations denoted by the thick orange curve.

One of the authors recently claimed that the one-loop inflationary tensor-power spectrum might be scale-invariantly enhanced or reduced due to a subhorizon resonant spectator scalar field [22]. Their reduction effect is due to the Born approximation for the fourth-order interaction Hamiltonian, which corresponds to the third-order source in the equation of motion in our analysis. The scale-invariant enhancement comes from the iterative correction of one-loop diagram (a1) in Fig. 2. The iterative correction during inflation can be amplified and dominant when the scalar Green function is also enhanced for a nontrivial background. We do not expect similar enhancement during radiation or matter eras. The iterative correction is comparable to the reduction effect in our case. In the present case, the coupling constant between ζ and h_{ij} is of the order of unity. Hence, the amplification of ζ always propagates to the loop. This is not necessarily the case during inflation in Ref. [22], since the coupling constant is slow-roll suppressed. Therefore, the inflationary one-loop correction is not necessarily enhanced for an arbitrary PBH formation scenario. However, the new significant reduction effect discussed in this paper always appears once ζ is amplified. Hence, PBH formation and reduction of primordial GWs may be two sides of the same coin, suggesting that combining GW detectors at all scales is indispensable!

ACKNOWLEDGMENTS

C. C., H.-Y. Z., and Y. H. Z. thank the Particle Cosmology Group at University of Science and Technology of China during their visits. A. O. would like to thank Keisuke Inomata, Misao Sasaki, and Yi Wang for useful discussions. We use the Mathematica package MathGR [110] in this work. This work is supported in part by the National Key R&D Program of China (Grant No. 2021YFC2203100). The authors are supported by the Jockey Club Institute for Advanced Study at

The Hong Kong University of Science and Technology. H.-Y. Z. is supported in part by a grant from the RGC of the Hong Kong SAR, China (Grant No. 16303220).

APPENDIX A: ITERATIVE SOLUTIONS IN THE IR REGION

In this appendix, we discuss the IR scaling of the three source terms we ignored in the main text. The first contribution arises from

$$S^{(3)}_{\phi h_{\phi h},ij} = 12\left[\phi h^{(2)\prime\prime}_{ij} + (2\mathcal{H}\phi + \phi')h^{(2)\prime}_{ij}\right]. \tag{A1}$$

The second-order tensor fluctuation in the above source is obtained by integrating

$$h^{(2)\prime\prime}_{ij} + 2\mathcal{H}h^{(2)\prime}_{ij} - \nabla^2 h^{(2)}_{ij} = 8\phi' h^{(1)\prime}_{ij} + 8\phi\nabla^2 h^{(1)}_{ij}. \tag{A2}$$

When substituting the solution of Eq. (A2) into Eq. (A1), we find the linear tensor fluctuation in the third-order source always appears with derivative operators. Then, from Eq. (18), those derivative operators turn into the external momentum when cross correlating with the linear field. Hence, these terms vanish in the IR region.

Secondly, we find the following source:

$$\begin{aligned} S^{(3)}_{h\phi_{\phi\phi},ij} &= 2h^{(1)}_{ij}(\nabla^2\Psi^{(2)} - \nabla^2\Phi^{(2)}) + 6(\Phi^{(2)} + \Psi^{(2)})\nabla^2 h^{(1)}_{ij} \\ &\quad + 3(\Phi^{(2)\prime} + 3\Psi^{(2)\prime})h^{(1)\prime}_{ij} + 3(\partial^k\Psi^{(2)} - \partial^k\Phi^{(2)}) \\ &\quad \times (\partial_j h^{(1)}_{ki} + \partial_i h^{(1)}_{kj} - \partial_k h^{(1)}_{ij}). \end{aligned} \tag{A3}$$

As discussed above, derivatives of tensor fluctuations will vanish in the IR region. In addition, the second-order scalar fluctuations in the first line of Eq. (A3) reduces to the zero modes so that $\nabla^2 = 0$. Therefore, we may safely ignore this source. Similarly, cross correlating $S^{(3)}_{hh_{\phi\phi},ij}$ with the linear tensor modes, $h_{\phi\phi}$ reduces to the zero mode, which should always be zero from statistical isotropy of cosmological perturbations.

APPENDIX B: ANALYTICAL RESULT IN RD

In this appendix, we provide the analytical expression for the kernel function generated from the source $S^{(3)}_{h\phi\phi}$ during RD era, which reads

$$\begin{aligned} I_{h,h\phi\phi}(u,x) = \frac{3}{70u^6x^2}\Bigg\{ & 2\sqrt{3}(53u^2-168)\sin 2x\,\mathrm{Si}\left(\frac{2ux}{\sqrt{3}}\right)u^5 + 2\sqrt{3}(53u^4-168u^2+630)u^3\log\left|\frac{\sqrt{3}u-3}{\sqrt{3}u+3}\right|\sin^2 x \\ & - 36(35u^6-70u^4+84u^2+36)\mathrm{Ci}(2x)\sin^2 x + 2(-53\sqrt{3}u^7+315u^6+168\sqrt{3}u^5-630u^4-630\sqrt{3}u^3 \\ & + 756u^2+324)\mathrm{Ci}\left(\frac{2}{3}|\sqrt{3}u-3|x\right)\sin^2 x + 2(53\sqrt{3}u^7+315u^6-168\sqrt{3}u^5-630u^4+630\sqrt{3}u^3 \\ & + 756u^2+324)\mathrm{Ci}\left(\frac{2}{3}(\sqrt{3}u+3)x\right)\sin^2 x - 18(35u^6-70u^4+84u^2+36)\log\left|\frac{u^2-3}{3}\right|\sin^2 x \\ & + \frac{6\sin x}{x^6}\Bigg[3x\cos x\Bigg(-70u^4x^4+84u^2x^4+36x^4+378u^2x^2-18x^2-3\sqrt{3}ux((9u^2-4)x^2+180)\sin\frac{2ux}{\sqrt{3}} \\ & + 810 + 2(2(13u^4-24u^2-9)x^4+9(9u^2+1)x^2-405)\cos\frac{2ux}{\sqrt{3}}\Bigg) + \sin x\Bigg(106u^6x^6+330u^4x^6 \\ & - 36u^2x^6-420u^4x^4+126u^2x^4+54x^4-2079u^2x^2-81x^2+\sqrt{3}ux(2(26u^4+57u^2-18)x^4 \\ & + 9(79u^2+6)x^2+1620)\sin\frac{2ux}{\sqrt{3}} - 3(2(26u^4+30u^2+9)x^4-9(17u^2+3)x^2-810)\cos\frac{2ux}{\sqrt{3}} - 2430\Bigg)\Bigg] \\ & + \sin 2x(53\sqrt{3}u^7-315u^6-168\sqrt{3}u^5+630u^4+630\sqrt{3}u^3-756u^2-324)\mathrm{Si}\left(\left(2-\frac{2u}{\sqrt{3}}\right)x\right) \\ & + 18\sin 2x(35u^6-70u^4+84u^2+36)\mathrm{Si}(2x) - \sin 2x(53\sqrt{3}u^7+315u^6-168\sqrt{3}u^5-630u^4 \\ & + 630\sqrt{3}u^3+756u^2+324)\mathrm{Si}\left(\frac{2}{3}(\sqrt{3}u+3)x\right)\Bigg\}. \end{aligned} \tag{B1}$$

[1] B. P. Abbott *et al.* (LIGO Scientific and Virgo Collaborations), Observation of Gravitational Waves from a Binary Black Hole Merger, Phys. Rev. Lett. **116**, 061102 (2016).

[2] B. P. Abbott *et al.* (LIGO Scientific and Virgo Collaborations), GW170817: Observation of Gravitational Waves from a Binary Neutron Star Inspiral, Phys. Rev. Lett. **119**, 161101 (2017).

[3] B. P. Abbott *et al.* (LIGO Scientific, Virgo, Fermi GBM, INTEGRAL, IceCube, AstroSat Cadmium Zinc Telluride Imager Team, IPN, Insight-Hxmt, ANTARES, Swift, AGILE Team, 1M2H Team, Dark Energy Camera GW-EM, DES, DLT40, GRAWITA, Fermi-LAT, ATCA, ASKAP, Las Cumbres Observatory Group, OzGrav, DWF (Deeper Wider Faster Program), AST3, CAASTRO, VINROUGE, MASTER, J-GEM, GROWTH, JAGWAR, CaltechNRAO, TTU-NRAO, NuSTAR, Pan-STARRS, MAXI Team, TZAC Consortium, KU, Nordic Optical Telescope, ePESSTO, GROND, Texas Tech University, SALT Group, TOROS, BOOTES, MWA, CALET, IKI-GW Follow-up, H.E.S.S., LOFAR, LWA, HAWC, Pierre Auger, ALMA, Euro VLBI Team, Pi of Sky, Chandra Team at McGill University, DFN, ATLAS Telescopes, High Time Resolution Universe Survey, RIMAS, RATIR, SKA South Africa/MeerKAT Collaborations), Multi-messenger observations of a binary neutron star merger, Astrophys. J. Lett. **848**, L12 (2017).

[4] Alan H. Guth, The inflationary universe: A possible solution to the horizon and flatness problems, Phys. Rev. D **23**, 347 (1981).

[5] Andrei D. Linde, A new inflationary universe scenario: A possible solution of the horizon, flatness, homogeneity, isotropy and primordial monopole problems, Phys. Lett. **108B**, 389 (1982).

[6] Alexei A. Starobinsky, A new type of isotropic cosmological models without singularity, Phys. Lett. **91B**, 99 (1980).

[7] Andreas Albrecht and Paul J. Steinhardt, Cosmology for Grand Unified Theories with Radiatively Induced Symmetry Breaking, Phys. Rev. Lett. **48**, 1220 (1982).

[8] Yi-Fu Cai, Shih-Hung Chen, James B. Dent, Sourish Dutta, and Emmanuel N. Saridakis, Matter bounce cosmology with the f(T) gravity, Classical Quantum Gravity **28**, 215011 (2011).

[9] Robert Brandenberger and Patrick Peter, Bouncing cosmologies: Progress and problems, Found. Phys. **47**, 797 (2017),

[10] Kevork Abazajian *et al.* (CMB-S4 Collaboration), CMB-S4: Forecasting constraints on primordial gravitational waves, Astrophys. J. **926**, 54 (2022).

[11] Kishore N. Ananda, Chris Clarkson, and David Wands, The cosmological gravitational wave background from primordial density perturbations, Phys. Rev. D **75**, 123518 (2007).

[12] Daniel Baumann, Paul J. Steinhardt, Keitaro Takahashi, and Kiyotomo Ichiki, Gravitational wave spectrum induced by primordial scalar perturbations, Phys. Rev. D **76**, 084019 (2007).

[13] Ryo Saito and Jun'ichi Yokoyama, Gravitational Wave Background as a Probe of the Primordial Black Hole Abundance, Phys. Rev. Lett. **102**, 161101 (2009); **107**, 069901(E) (2011).

[14] Keisuke Inomata, Masahiro Kawasaki, Kyohei Mukaida, Yuichiro Tada, and Tsutomu T. Yanagida, Inflationary primordial black holes for the LIGO gravitational wave events and pulsar timing array experiments, Phys. Rev. D **95**, 123510 (2017).

[15] Kazunori Kohri and Takahiro Terada, Semianalytic calculation of gravitational wave spectrum nonlinearly induced from primordial curvature perturbations, Phys. Rev. D **97**, 123532 (2018).

[16] N. Bartolo, V. De Luca, G. Franciolini, M. Peloso, D. Racco, and A. Riotto, Testing primordial black holes as dark matter with LISA, Phys. Rev. D **99**, 103521 (2019).

[17] Yi-Fu Cai, Chao Chen, Xi Tong, Dong-Gang Wang, and Sheng-Feng Yan, When primordial black holes from sound speed resonance meet a stochastic background of gravitational waves, Phys. Rev. D **100**, 043518 (2019).

[18] Juan Garcia-Bellido, Marco Peloso, and Caner Unal, Gravitational wave signatures of inflationary models from primordial black hole dark matter, J. Cosmol. Astropart. Phys. 09 (2017) 013.

[19] Keisuke Inomata, Analytic solutions of scalar perturbations induced by scalar perturbations, J. Cosmol. Astropart. Phys. 03 (2021) 013.

[20] Guillem Domènech, Scalar induced gravitational waves review, Universe **7**, 398 (2021).

[21] Rong-Gen Cai, Chao Chen, and Chengjie Fu, Primordial black holes and stochastic gravitational wave background from inflation with a noncanonical spectator field, Phys. Rev. D **104**, 083537 (2021).

[22] Atsuhisa Ota, Misao Sasaki, and Yi Wang, Scale-invariant enhancement of gravitational waves during inflation, arXiv:2209.02272.

[23] Rong-gen Cai, Shi Pi, and Misao Sasaki, Gravitational Waves Induced by non-Gaussian Scalar Perturbations, Phys. Rev. Lett. **122**, 201101 (2019).

[24] Caner Unal, Imprints of primordial non-gaussianity on gravitational wave spectrum, Phys. Rev. D **99**, 041301 (2019).

[25] Peter Adshead, Kaloian D. Lozanov, and Zachary J. Weiner, Non-Gaussianity and the induced gravitational wave background, J. Cosmol. Astropart. Phys. 10 (2021) 080.

[26] Sebastian Garcia-Saenz, Lucas Pinol, Sébastien Renaux-Petel, and Denis Werth, No-go theorem for scalar-trispectrum-induced gravitational waves, arXiv:2207.14267.

[27] Keisuke Inomata and Tomohiro Nakama, Gravitational waves induced by scalar perturbations as probes of the small-scale primordial spectrum, Phys. Rev. D **99**, 043511 (2019).

[28] H. V. Ragavendra, Accounting for scalar non-Gaussianity in secondary gravitational waves, Phys. Rev. D **105**, 063533 (2022).

[29] Jacopo Fumagalli, Sébastien Renaux-Petel, and Lukas T. Witkowski, Oscillations in the stochastic gravitational wave background from sharp features and particle production during inflation, J. Cosmol. Astropart. Phys. 08 (2021) 030.

[30] Matteo Braglia, Xingang Chen, and Dhiraj Kumar Hazra, Probing primordial features with the stochastic gravitational wave background, J. Cosmol. Astropart. Phys. 03 (2021) 005.

[31] Jacopo Fumagalli, S. ébastien Renaux-Petel, and Lukas T. Witkowski, Resonant features in the stochastic gravitational wave background, J. Cosmol. Astropart. Phys. 08 (2021) 059.
[32] Atsuhisa Ota, Induced superhorizon tensor perturbations from anisotropic non-Gaussianity, Phys. Rev. D **101**, 103511 (2020).
[33] Vicente Atal and Guillem Domènech, Probing non-Gaussianities with the high frequency tail of induced gravitational waves, J. Cosmol. Astropart. Phys. 06 (2021) 001.
[34] Ema Dimastrogiovanni, Matteo Fasiello, Ameek Malhotra, and Gianmassimo Tasinato, Enhancing gravitational wave anisotropies with peaked scalar sources, J. Cosmol. Astropart. Phys. 01 (2023) 018.
[35] Chao Chen and Atsuhisa Ota, Induced gravitational waves from statistically anisotropic scalar perturbations, Phys. Rev. D **106**, 063507 (2022).
[36] Stephen Hawking, Gravitationally collapsed objects of very low mass, Mon. Not. R. Astron. Soc. **152**, 75 (1971).
[37] Bernard J. Carr and S. W. Hawking, Black Holes in the Early Universe, Mon. Not. R. Astron. Soc. **168**, 399 (1974).
[38] Bernard J. Carr, The primordial black hole mass spectrum, Astrophys. J. **201**, 1 (1975).
[39] Juan Garcia-Bellido and Ester Ruiz Morales, Primordial black holes from single field models of inflation, Phys. Dark Universe **18**, 47 (2017).
[40] Cristiano Germani and Tomislav Prokopec, On primordial black holes from an inflection point, Phys. Dark Universe **18**, 6 (2017).
[41] Christian T. Byrnes, Philippa S. Cole, and Subodh P. Patil, Steepest growth of the power spectrum and primordial black holes, J. Cosmol. Astropart. Phys. 06 (2019) 028.
[42] Jing Liu, Zong-Kuan Guo, and Rong-Gen Cai, Analytical approximation of the scalar spectrum in the ultraslow-roll inflationary models, Phys. Rev. D **101**, 083535 (2020).
[43] Chengjie Fu, Puxun Wu, and Hongwei Yu, Primordial black holes and oscillating gravitational waves in slow-roll and slow-climb inflation with an intermediate noninflationary phase, Phys. Rev. D **102**, 043527 (2020).
[44] Keisuke Inomata, Evan McDonough, and Wayne Hu, Amplification of primordial perturbations from the rise or fall of the inflaton, J. Cosmol. Astropart. Phys. 02 (2022) 031.
[45] Gianmassimo Tasinato, An analytic approach to non-slow-roll inflation, Phys. Rev. D **103**, 023535 (2021).
[46] Ogan Özsoy and Gianmassimo Tasinato, Consistency conditions and primordial black holes in single field inflation, Phys. Rev. D **105**, 023524 (2022).
[47] Philippa S. Cole, Andrew D. Gow, Christian T. Byrnes, and Subodh P. Patil, Steepest Growth Re-Examined: Repercussions for Primordial Black Hole Formation, arXiv:2204.07573.
[48] Kazunori Kohri, Chia-Min Lin, and Tomohiro Matsuda, Primordial black holes from the inflating curvaton, Phys. Rev. D **87**, 103527 (2013).
[49] Masahiro Kawasaki, Naoya Kitajima, and Tsutomu T. Yanagida, Primordial black hole formation from an axion-like curvaton model, Phys. Rev. D **87**, 063519 (2013).
[50] Shi Pi, Ying-li Zhang, Qing-Guo Huang, and Misao Sasaki, Scalaron from R^2-gravity as a heavy field, J. Cosmol. Astropart. Phys. 05 (2018) 042.
[51] Lilia Anguelova, On primordial black holes from rapid turns in two-field models, J. Cosmol. Astropart. Phys. 06 (2021) 004.
[52] Gonzalo A. Palma, Spyros Sypsas, and Cristobal Zenteno, Seeding Primordial Black Holes in Multifield Inflation, Phys. Rev. Lett. **125**, 121301 (2020).
[53] Jacopo Fumagalli, Sébastien Renaux-Petel, John W. Ronayne, and Lukas T. Witkowski, Turning in the landscape: A new mechanism for generating primordial black holes, arXiv:2004.08369.
[54] Shi Pi and Misao Sasaki, Primordial black hole formation in non-minimal curvaton scenario, arXiv:2112.12680.
[55] Jose María Ezquiaga, Juan García-Bellido, and Vincent Vennin, The exponential tail of inflationary fluctuations: consequences for primordial black holes, J. Cosmol. Astropart. Phys. 03 (2020) 029.
[56] Vicente Atal, Judith Cid, Albert Escrivà, and Jaume Garriga, PBH in single field inflation: The effect of shape dispersion and non-Gaussianities, J. Cosmol. Astropart. Phys. 05 (2020) 022.
[57] Daniel G. Figueroa, Sami Raatikainen, Syksy Rasanen, and Eemeli Tomberg, Non-Gaussian Tail of the Curvature Perturbation in Stochastic Ultraslow-Roll Inflation: Implications for Primordial Black Hole Production, Phys. Rev. Lett. **127**, 101302 (2021).
[58] Yi-Fu Cai, Xiao-Han Ma, Misao Sasaki, Dong-Gang Wang, and Zihan Zhou, One small step for an inflaton, one giant leap for inflation: A novel non-gaussian tail and primordial black holes, Phys. Lett. B **834**, 137461 (2022).
[59] Yi-Fu Cai, Xiao-Han Ma, Misao Sasaki, Dong-Gang Wang, and Zihan Zhou, Highly non-gaussian tails and primordial black holes from single-field inflation, J. Cosmol. Astropart. Phys. 12 (2022) 034.
[60] Takahiko Matsubara and Misao Sasaki, Non-gaussianity effects on the primordial black hole abundance for sharply-peaked primordial spectrum, arXiv:2208.02941.
[61] Yi-Fu Cai, Xi Tong, Dong-Gang Wang, and Sheng-Feng Yan, Primordial Black Holes from Sound Speed Resonance during Inflation, Phys. Rev. Lett. **121**, 081306 (2018).
[62] Chao Chen and Yi-Fu Cai, Primordial black holes from sound speed resonance in the inflaton-curvaton mixed scenario, J. Cosmol. Astropart. Phys. 10 (2019) 068.
[63] Chao Chen, Xiao-Han Ma, and Yi-Fu Cai, Dirac-Born-Infeld realization of sound speed resonance mechanism for primordial black holes, Phys. Rev. D **102**, 063526 (2020).
[64] Zihan Zhou, Jie Jiang, Yi-Fu Cai, Misao Sasaki, and Shi Pi, Primordial black holes and gravitational waves from resonant amplification during inflation, Phys. Rev. D **102**, 103527 (2020).
[65] Zhi-Zhang Peng, Chengjie Fu, Jing Liu, Zong-Kuan Guo, and Rong-Gen Cai, Gravitational waves from resonant amplification of curvature perturbations during inflation, J. Cosmol. Astropart. Phys. 10 (2021) 050.
[66] Andrea Addazi, Salvatore Capozziello, and Qingyu Gan, Induced gravitational waves from multi-sound speed resonances during cosmological inflation, J. Cosmol. Astropart. Phys. 08 (2022) 051.

[67] Amjad Ashoorioon, Abasalt Rostami, and Javad T. Firouzjaee, EFT compatible PBHs: Effective spawning of the seeds for primordial black holes during inflation, J. High Energy Phys. 07 (2021) 087.
[68] Pau Amaro-Seoane *et al.* (LISA Collaboration), Laser interferometer space antenna, arXiv:1702.00786.
[69] Seiji Kawamura *et al.*, The Japanese space gravitational wave antenna: DECIGO, Classical Quantum Gravity **28**, 094011 (2011).
[70] Wen-Hong Ruan, Zong-Kuan Guo, Rong-Gen Cai, and Yuan-Zhong Zhang, Taiji program: Gravitational-wave sources, Int. J. Mod. Phys. A **35**, 2050075 (2020).
[71] Jun Luo *et al.* (TianQin Collaboration), TianQin: A space-borne gravitational wave detector, Classical Quantum Gravity **33**, 035010 (2016).
[72] Chen Yuan, Zu-Cheng Chen, and Qing-Guo Huang, Probing primordial–black-hole dark matter with scalar induced gravitational waves, Phys. Rev. D **100**, 081301 (2019).
[73] Jing-Zhi Zhou, Xukun Zhang, Qing-Hua Zhu, and Zhe Chang, The third order scalar induced gravitational waves, J. Cosmol. Astropart. Phys. 05 (2022) 013.
[74] Zhe Chang, Xukun Zhang, and Jing-Zhi Zhou, The cosmological vector modes from a monochromatic primordial power spectrum, J. Cosmol. Astropart. Phys. 10 (2022) 084.
[75] Jinn-Ouk Gong, Analytic integral solutions for induced gravitational waves, Astrophys. J. **925**, 102 (2022).
[76] Zhe Chang, Xukun Zhang, and Jing-Zhi Zhou, Gravitational waves from primordial scalar and tensor perturbations, Phys. Rev. D **107**, 063510 (2023).
[77] F. Bernardeau, S. Colombi, E. Gaztanaga, and R. Scoccimarro, Large scale structure of the universe and cosmological perturbation theory, Phys. Rep. **367**, 1 (2002).
[78] Martin Crocce and Roman Scoccimarro, Renormalized cosmological perturbation theory, Phys. Rev. D **73**, 063519 (2006).
[79] Teresa Hui-Ching Lu, Kishore Ananda, and Chris Clarkson, Vector modes generated by primordial density fluctuations, Phys. Rev. D **77**, 043523 (2008).
[80] Juan Martin Maldacena, Non-Gaussian features of primordial fluctuations in single field inflationary models, J. High Energy Phys. 05 (2003) 013.
[81] José Ramón Espinosa, Davide Racco, and Antonio Riotto, A cosmological signature of the SM Higgs instability: Gravitational waves, J. Cosmol. Astropart. Phys. 09 (2018) 012.
[82] Rong-Gen Cai, Shi Pi, and Misao Sasaki, Universal infrared scaling of gravitational wave background spectra, Phys. Rev. D **102**, 083528 (2020).
[83] Wayne T. Hu, Wandering in the Background: A CMB Explorer, Other thesis, University of California, Berkerley, 1995, arXiv:astro-ph/9508126.
[84] Simeon Bird, Ilias Cholis, Julian B. Muñoz, Yacine Ali-Haïmoud, Marc Kamionkowski, Ely D. Kovetz, Alvise Raccanelli, and Adam G. Riess, Did LIGO Detect Dark Matter?, Phys. Rev. Lett. **116**, 201301 (2016).
[85] Misao Sasaki, Teruaki Suyama, Takahiro Tanaka, and Shuichiro Yokoyama, Primordial Black Hole Scenario for the Gravitational-Wave Event GW150914, Phys. Rev. Lett. **117**, 061101 (2016); **121**, 059901(E) (2018).
[86] Anne M. Green and Bradley J. Kavanagh, Primordial black holes as a dark matter candidate, J. Phys. G **48**, 043001 (2021).
[87] Atsuhisa Ota, Misao Sasaki, and Yi Wang, One-loop tensor power spectrum from an excited scalar field during inflation, arXiv:2211.12766.
[88] Hooshyar Assadullahi and David Wands, Gravitational waves from an early matter era, Phys. Rev. D **79**, 083511 (2009).
[89] Laila Alabidi, Kazunori Kohri, Misao Sasaki, and Yuuiti Sendouda, Observable induced gravitational waves from an early matter phase, J. Cosmol. Astropart. Phys. 05 (2013) 033.
[90] Keisuke Inomata, Kazunori Kohri, Tomohiro Nakama, and Takahiro Terada, Enhancement of gravitational waves induced by scalar perturbations due to a sudden transition from an early matter era to the radiation era, Phys. Rev. D **100**, 043532 (2019).
[91] Keisuke Inomata, Kazunori Kohri, Tomohiro Nakama, and Takahiro Terada, Gravitational waves induced by scalar perturbations during a transition from an early matter era to the radiation era, J. Cosmol. Astropart. Phys. 10 (2019) 071.
[92] Ioannis Dalianis and Chris Kouvaris, Gravitational waves from density perturbations in an early matter domination era, J. Cosmol. Astropart. Phys. 07 (2021) 046.
[93] M. Hazumi *et al.* (LiteBIRD Collaboration), LiteBIRD: JAXA's new strategic L-class mission for all-sky surveys of cosmic microwave background polarization, Proc. SPIE Int. Soc. Opt. Eng. **11443**, 114432F (2020).
[94] Y. Akrami *et al.* (Planck Collaboration), Planck 2018 Results. X. Constraints on Inflation, Astron. Astrophys. **641**, A10 (2020).
[95] J. CHLuba *et al.*, New horizons in cosmology with spectral distortions of the cosmic microwave background, Exper. Astron. **51**, 1515 (2021).
[96] Misao Sasaki, Teruaki Suyama, Takahiro Tanaka, and Shuichiro Yokoyama, Primordial black holes–perspectives in gravitational wave astronomy, Classical Quantum Gravity **35**, 063001 (2018).
[97] Simeon Bird, Hiranya V. Peiris, Matteo Viel, and Licia Verde, Minimally parametric power spectrum reconstruction from the Lyman-Alpha forest, Mon. Not. R. Astron. Soc. **413**, 1717 (2011).
[98] D. J. Fixsen, E. S. Cheng, J. M. Gales, John C. Mather, R. A. Shafer, and E. L. Wright, The cosmic microwave background spectrum from the full cobe FIRAS data set, Astrophys. J. **473**, 576 (1996).
[99] Keisuke Inomata and Takahiro Terada, Gauge independence of induced gravitational waves, Phys. Rev. D **101**, 023523 (2020).
[100] V. De Luca, G. Franciolini, A. Kehagias, and A. Riotto, On the gauge invariance of cosmological gravitational waves, J. Cosmol. Astropart. Phys. 03 (2020) 014.
[101] Guillem Domènech and Misao Sasaki, Approximate gauge independence of the induced gravitational wave spectrum, Phys. Rev. D **103**, 063531 (2021).
[102] Atsuhisa Ota, Hayley J. Macpherson, and William R. Coulton, Covariant transverse-traceless projection for

secondary gravitational waves, Phys. Rev. D **106**, 063521 (2022).
[103] Enrico Pajer and Matias Zaldarriaga, A New Window on Primordial Non-Gaussianity, Phys. Rev. Lett. **109**, 021302 (2012).
[104] Jonathan Ganc and Eiichiro Komatsu, Scale-dependent bias of galaxies and Mu-type distortion of the cosmic microwave background spectrum from single-field inflation with a modified initial state, Phys. Rev. D **86**, 023518 (2012).
[105] Atsuhisa Ota, Cosmological constraints from μE cross-correlations, Phys. Rev. D **94**, 103520 (2016).
[106] Atsuhisa Ota, Toyokazu Sekiguchi, Yuichiro Tada, and Shuichiro Yokoyama, Anisotropic Cmb Distortions from non-gaussian isocurvature perturbations, J. Cosmol. Astropart. Phys. 03 (2015) 013.
[107] Atsuhisa Ota and Masahide Yamaguchi, Secondary isocurvature perturbations from acoustic reheating, J. Cosmol. Astropart. Phys. 06 (2018) 022.
[108] Atsushi Naruko, Atsuhisa Ota, and Masahide Yamaguchi, Probing small-scale non-gaussianity from anisotropies in acoustic reheating, J. Cosmol. Astropart. Phys. 05 (2015) 049.
[109] Donghui Jeong, Jinn-Ouk Gong, Hyerim Noh, and Jaichan Hwang, General relativistic effects on non-linear power spectra, Astrophys. J. **727**, 22 (2011).
[110] Yi Wang, MathGR: A tensor and GR computation package to keep it simple, arXiv:1306.1295.